ChemPubSoc Europe

DOI: 10.1002/chem.201403130

CHEMISTRY
A European Journal
Communication

Self-Assembly

Drug Conjugation to Cyclic Peptide–Polymer Self-Assembling Nanotubes

Bianca M. Blunden,[a, b] Robert Chapman,[c] Maarten Danial,[c] Hongxu Lu,[a] Katrina A. Jolliffe,*[d] Sébastien Perrier,*[c, e, f] and Martina H. Stenzel*[a]

Abstract: We show for the first time how polymeric nanotubes (NTs) based on self-assembled conjugates of polymers and cyclic peptides can be used as an efficient drug carrier. RAPTA-C, a ruthenium-based anticancer drug, was conjugated to a statistical co-polymer based on poly(2-hydroxyethyl acrylate) (pHEA) and poly(2-chloroethyl methacrylate) (pCEMA), which formed the shell of the NTs. Self-assembly into nanotubes (length 200–500 nm) led to structures exhibiting high activity against cancer cells.

Nanotechnology has had a tremendous impact on the medical field, in particular through the development of nanoscale systems for the enhancement of drug action. For instance, drug nanocarriers have dramatically improved the efficiency of drugs, because they optimize biodistribution and prevent rapid metabolization or excretion from the body.[1] Materials and pharmaceuticals science have joined forces to deliver a broad range of nanomaterials with diverse size, architectures, and functionality, such as: liposomes, dendrimers, inorganic and organic particles.[2] The latter have especially received much attention: the particles size and functionality can be finely tuned, thus allowing control over their pharmacokinetics and biodistribution. Recent work has demonstrated that their shape plays an important role in their biological properties and particle shape affects their transport in the body, for instance, through orientation and mechanical stiffness.[3] This provides new opportunities to fine tune the particles properties. Targeting ability can also be directed by shape, through control of the overall surface area and local curvature. Tubular structures are particularly exciting nanomaterials to be used as delivery vectors, because their elongated shape allows them to circulate to areas, which spherical nanoparticles of equivalent volume could not reach, whilst maximizing their surface contact area to attach to the desired location.

Among the many examples of natural and artificial nanotubes (NTs),[4] cyclic peptide-based nanotubes form one of the most versatile and functional family of such materials. NTs are obtained by the stacking of cyclic peptides containing 6–12 amino acids of alternating D and L chirality, through antiparallel β-sheet hydrogen bonding.[5] The extended hydrogen bonding allows the formation of rigid tube-like structures, which typically extend well over 100 nm. The structures are stable against proteases due to their cyclic structure and the incorporation of D-amino acid residues, but disassemble under specific (acidic) conditions.[6] Very recent developments in the field have shown that the grafting of polymers to these peptide NTs prevent their aggregation and improve their stability and solubility, without distorting the tubular structure.[7] Grafting polymeric chains to the cyclic peptides also gives a degree of length control of the nanotubes,[6,8] as well as a mode of introducing functionality.[9] The conjugation of polymers to cyclic peptides lead to functional NTs that present additional advantages for drug delivery over typical spherical nanoparticles, because they can span a large area on cells and provide multivalent drug display and/or release.[10] In addition, the high aspect ratio can enhance the circulation time in the body,[11] while the nanosize promotes the lodgement of the drug carrier in the tumor.[12] The functional polymer shell also provides an ample opportunity to conjugate a drug and the drug carrier can potentially disassemble through hydrogen-bond breakage, thus allowing better clearance. Although polymer-coated peptide-based nanotubes appear to be highly suitable materials for the delivery of drugs, they have only barely been exploited for this purpose. One recent example is the use of polyethylene glycol (PEG)-coated NTs for the delivery of doxorubicin.[13]

The ability to form drug conjugates paired with the potentially slow disassembly could make peptide nanotubes the drug carrier of choice when attempting to transport therapeu-

[a] Dr. B. M. Blunden, Dr. H. Lu, Prof. M. H. Stenzel
Centre for Advanced Macromolecular Design, School of Chemistry
University of New South Wales, Sydney, NSW 2052 (Australia)
E-mail: M.Stenzel@unsw.edu.au

[b] Dr. B. M. Blunden
Cooperative Research Centre (CRC) for Polymers
8 Redwood Drive, Notting Hill, Victoria 3618 (Australia)

[c] Dr. R. Chapman, Dr. M. Danial, Prof. S. Perrier
Key Centre for Polymers and Colloids, School of Chemistry
The University of Sydney, Sydney, NSW 2006 (Australia)

[d] Prof. K. A. Jolliffe
School of Chemistry, The University of Sydney
Sydney, NSW 2006 (Australia)
E-mail: kate.jolliffe@sydney.edu.au

[e] Prof. S. Perrier
Department of Chemistry, The University of Warwick
Coventry CV4 7AL (UK)
E-mail: S.Perrier@warwick.ac.uk

[f] Prof. S. Perrier
Faculty of Pharmacy and Pharmaceutical Sciences
Monash University, 381 Royal Parade, Parkville, VIC 3052 (Australia)

Supporting information for this article is available on the WWW under http://dx.doi.org/10.1002/chem.201403130. It contains the experimental details.

tics that cannot be delivered by using traditional encapsulation techniques. Examples of such challenging systems are metal-based drugs, which are often neither hydrophilic nor hydrophobic enough to be encapsulated in a compatible polymer matrix.[14] Of particular interest is the ruthenium metallodrug RAPTA-C [rutheniumdichloride(*p*-cymene)PTA], in which PTA = 1,3,5-triaza-7-phosphaadamantane, which is weakly cytotoxic in vitro but very selective and efficient on metastases in vivo.[15] The drug is not very effective against primary tumors,[16] but has shown to be active on metastases.[15f,17] RAPTA-C significantly inhibits the progression of cancer in animal models, by reducing the number and weight of solid metastases, with low general toxicity.[16] Despite these advantages, RAPTA-C faces challenges that are typical to many drugs of its class, which include low solubility and degradation prior to reaching the target. Many of these challenges can be addressed by attaching the drug to a polymer carrier forming a macromolecular metal complex.[14]

Herein, we demonstrate the feasibility of peptide nanotubes as a carrier for the delivery of drugs, exemplified by using RAPTA-C. Water-soluble polymers, based herein on poly(2-hydroxyethyl acrylate) (pHEA), was grafted to the cyclic peptide. Copolymerization with 2-chloroethyl methacrylate (CEMA) gave reactive polymers that can generate a handle for the conjugation of drugs. Subsequent self-assembly into peptide nanotubes resulted in the formation of the nanosized carrier (Scheme 1).

Poly(2-hydroxyethyl acrylate) (pHEA) has previously been shown to improve the solubility of cyclic peptide conjugates, and the resulting nanotubes, in polar solvents such as water.[6] HEA has also been copolymerized with CEMA.[18] Copolymerization with CEMA gave a conjugation avenue for the ruthenium anticancer therapeutic RAPTA-C through a substitution reaction of the halogen with the amide of the PTA (1,3,5-triaza-phosphaadamantane) ligand.[19] Thus, by conjugation of this polymer to a cyclic peptide, we hypothesized that it should be possible to attach RAPTA-C to a water-soluble nanoscale drug carrier.

To this end, HEA and CEMA were copolymerized by using the alkyne functional RAFT agent depicted in Scheme 1, resulting in a statistical co-polymer with a terminal alkyne group. The polymerization proceeded with linear pseudo-first-order kinetics, and gave polymeric chains with high end-group fidelity, as was confirmed by using ^{1}H NMR (Figure S1 in the Supporting Information) and narrow molecular-weight distributions (Figures S2 and S3 in the Supporting Information). Detailed studies revealed a slight gradient structure of the polymer with a preference for incorporation of CEMA in the initial stages of the polymerization (Figure S4 in the Supporting Information). More detailed analysis of this polymerization can be found elsewhere.[18]

One polymer, p(HEA_{58}-co-$CEMA_{10}$), was isolated for further work. The polymer was coupled to a cyclic peptide bearing two azidolysine side chains [CP-$(N_3)_2$] using a previously established microwave assisted, copper-catalyzed azide–alkyne cycloaddition (CuAAC) method.[20] Excess polymer was removed by preparative size-exclusion chromatography (SEC) over sephadex. The analytical SEC trace after purification showed a clear shift in the molecular weight of the polymer after conjugation to the peptide (Figure S5 in the Supporting Information). The high molecular-weight broadening is indicative of a small amount of aggregation of the conjugates into dimers and trimers during analysis.[7b] Complete conversion of the azide groups on the peptide was evidenced by the FTIR spectrum, which showed no residual azide at 2095 cm^{-1} after conjugation (Figure S6 in the Supporting Information). The appearance of a signal attributable to the polymer carbonyl stretch and more intense C–H stretches, due to the increase in the number of C–H bonds present in the polymer conjugate, are also evident.

The conjugated peptide (CP-p(HEA-CEMA)$_2$) then underwent a Finkelstein reaction[21] to convert the chloride end groups of the CEMA monomer to iodide end groups. This was necessary to increase the reactivity of the halogen to facilitate the reaction with PTA.[18] This substitution was confirmed by ^{1}H NMR, in which the signal corresponding to CH_2–Cl at $\delta = 3.80$ ppm shifted upfield to 3.40 ppm, when the chloride was substituted with iodide. This signal could be monitored relative to the adjoining CH_2 signal at 4.23 ppm, which did not shift. RAPTA-C was then attached to the polymer by using the method detailed in previous work.[18] PTA was first attached to the peptide–polymer conjugate through reaction of the iodide side

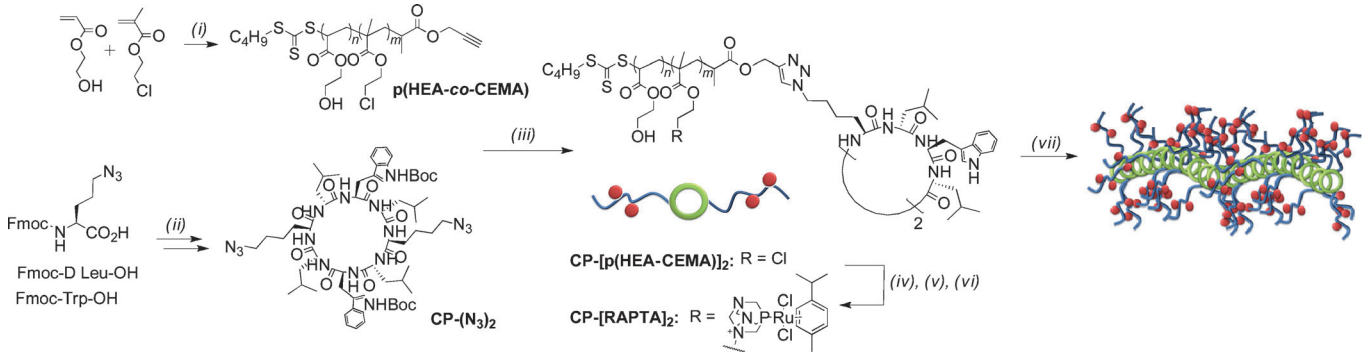

Scheme 1. Synthesis of cyclic peptide–polymer conjugate CP-[p(HEA-CEMA)$_2$] and attachment of RAPTA-C to form CP-[RAPTA]$_2$. i) RAFT co-polymerization of HEA and CEMA, DMAc, 60 °C, 24 h; ii) solid-phase peptide synthesis and cyclisation in DMF; iii) Na ascorbate, $CuSO_4$, DMF/TFE, 100 °C, 15 min, μw; iv) NaI, 70 °C; v) PTA, DMSO, 25 °C; vi) [$RuCl_2$(*p*-cymene)] dimer; vii) self-assembly in DMSO and water.

chains with the free amine to give the quaternary ammonium species, as was evidenced by a shift in the ^{31}P NMR signal for the PTA phosphorus atom from −103 to −84 ppm[22] (Figure S7 in the Supporting Information, bottom). The ruthenium dimer was subsequently added to give the polymer-conjugated RAPTA-C (CP-P(HEA_{58}-((RAPTA-C)-EMA)$_{10}$)$_2$. A very large deshielding of the corresponding signal in the ^{31}P NMR spectrum was observed, shown by the peak shift to −18 ppm (Figure S7 in the Supporting Information, top). These values were consistent with the conjugation to the homopolymer.[18] As was found previously,[18] the polymer–PTA and polymer–RAPTA-C peaks were broad, due to the inherent rigidity of polymers. Furthermore, the residual unreacted PTA underwent a complexation reaction producing RAPTA-C on addition of the $RuCl_2$(*p*-cymene) dimer, shown by the ^{31}P chemical shift at −103 moving to −33 ppm.

A highly complex ^1H NMR spectra with multiple spin systems resulted from the *N*-alkylation of PTA due to the decrease in molecular symmetry.[23] Due to the combined characteristic broadening from the conjugate, the ^1H spectrum is difficult to interpret. However, the *p*-cymene region for the reaction provided further evidence for the conjugation reaction, because the peaks for the residual unreacted $RuCl_2$(*p*-cymene) dimer, RAPTA-C and the broad peak for the conjugated RAPTA-C are evident (Figure S8 in the Supporting Information). Also, consistent with earlier work,[18] the first step was found to be the rate-limiting step in the conjugation. All conjugated and unconjugated PTA was consumed during the RAPTA-C complexation, giving both free RAPTA-C and conjugated RAPTA-C. Small side-products evident in the ^{31}P spectra, apart from the phosphorous oxide peak previously observed, are most likely the hydrolysis products due to the exchange of the RAPTA-C chloride ligands with hydroxide and water.

After drug conjugation, the DMSO solution was diluted with water, and the mixture was dialyzed to remove DMSO, unconjugated RAPTA-C, and phosphorous oxide. The red color of the resulting solution is indicative of the attachment of RAPTA-C. The amount of conjugated RAPTA-C was quantified by using inductively coupled plasma mass spectrometry (ICPMS) resulting in a Ru concentration of 5×10^{-2} mmol L^{-1} of the solution shown in Figure 1. Self-assembly of the conjugates into nanotubes was investigated by using both static and dynamic light scattering (SLS and DLS, respectively), as well as transmission electron microscopy (TEM). DLS of the NTs in both DMSO and water confirmed the presence of large aggregates, 500–1000 nm in hydrodynamic diameter, indicative of the formation of nanotubes in both cases (Figure 1). SLS data provided an initial estimate of the shape of the aggregates by measurement of the radius of gyration (r_g). The RAPTA-C conjugates gave form factors (r_g/r_h) of greater than one (Figure S9 in the Supporting Information), suggesting the aggregates observed by DLS are indeed extended tubes.

TEM was used to provide further characterization of the nanotubes, although obtaining images of the tubes in dried films can be difficult. We presume the dynamic nature of the assembly can cause disruption of the hydrogen bonding between the peptide units, which results in the dissociation of

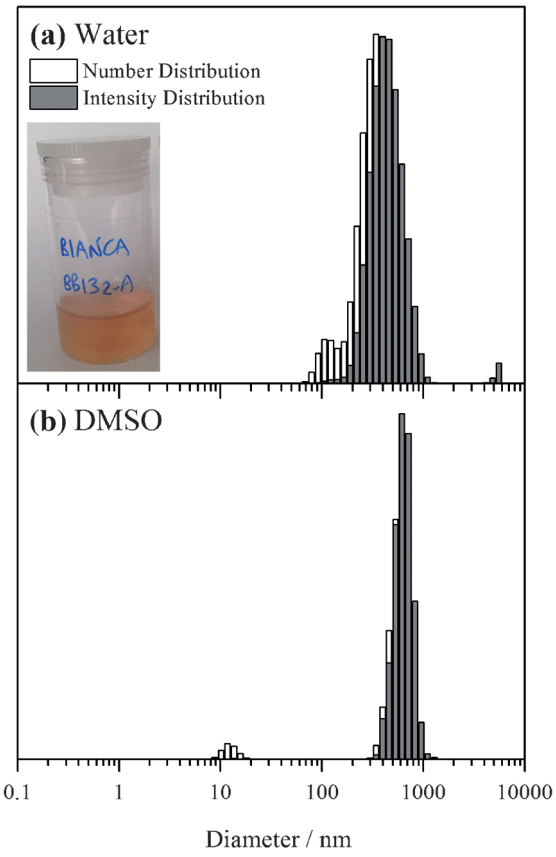

Figure 1. DLS intensity and number particle-size distributions at 25 °C in a) water after dialysis and b) DMSO.

the tubes upon drying. However, the NTs were still visible under these conditions (Figure 2 a and b). Better representation of the structures in solution can be achieved by crosslinking of the NTs prior to drying. The NTs were crosslinked by reaction of the OH functionality on the HEA units with toluene diisocyanate, thus "locking in" the structure, as has been shown previously.[6] These crosslinked conjugates were much easier to image by TEM (Figure 2 c–f). An abundance of rod-like structures between 200 and 500 nm in length, and approximately 20 nm in diameter, were observed by TEM in dried films. These results correspond well with the DLS and SLS measurements and confirm the presence of tubes in solution. In an attempt to image the uncrosslinked RAPTA-C containing NT's in solution, the polymers were labelled with fluorescein isothiocyanate (FITC), and the uncrosslinked NTs were imaged by using confocal fluorescent microscopy (Figure 2 f). Despite a size that is close to the limit of resolution of the instrument, the FITC-tagged NTs could still be observed. The scale bar in Figure 2 f is 2 μm, and the features seen are around 200–500 nm in length, similar to the TEM pictures. It should be noted here that the confocal fluorescent microscopy showed the uncrosslinked NTs in aqueous solution, and are therefore an indication of the real structure.

The assembled NT's were tested against ovarian A2780 and cisplatin-resistant ovarian A2780cis cancer-cell lines, and their efficacy was compared with the pure drug RAPTA-C. Nano-

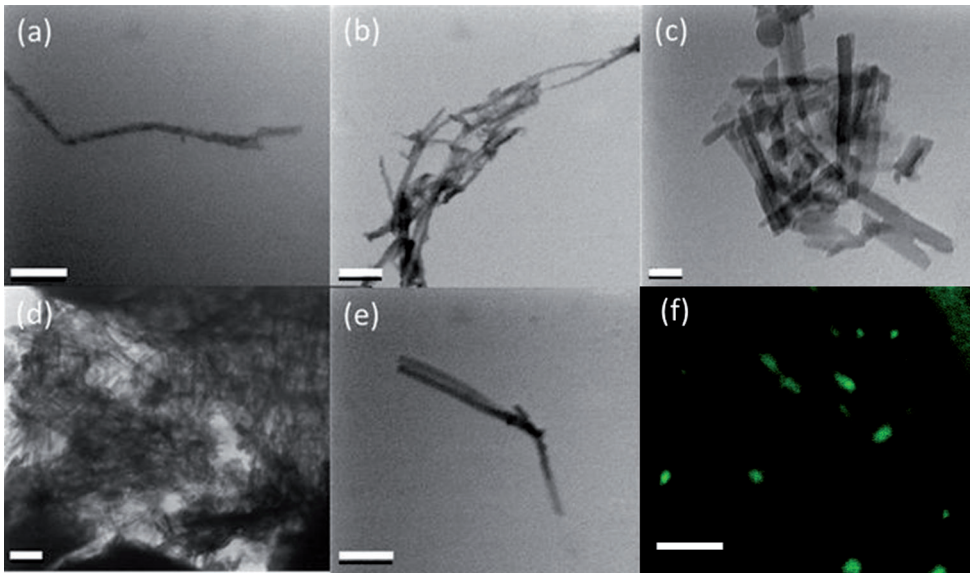

Figure 2. TEM a) and b) CP-P(HEA_{58}-((RAPTA-C)-$EMA)_{10})_2$, c)–e) crosslinked CP P(HEA_{58}-((RAPTA-C)-$EMA)_{10})_2$. Samples a)–d) were drop loaded onto grid, air dried, and stained with osmium tetroxide. Sample e) was drop loaded onto grid and air dried. f) Confocal fluorescent micrograph taken of a solution in water; scale bars: a) and e) = 100 nm; b), d), and f) = 200 nm; c) = 50 nm, and f) = 2 μm.

with a high aspect ratio may have clear advantages when it comes to an extended circulation time in the blood stream.[11]

In conclusion, cyclic peptide–polymer nanotubes were identified as an appropriate drug carrier for RAPTA-C. A co-polymer containing HEA (for solubility) and CEMA (for conjugation) was designed to increase solubility of the peptides and allow conjugation of RAPTA-C. The co-polymer was prepared and successfully conjugated to self-assembling cyclic peptides. The drug was also successfully conjugated without disrupting the self-assembly of the conjugates into nanotubes, as was shown by DLS and TEM. A tenfold increase in cytotoxicity was found for NTs with bound RAPTA-C, compared with the free drug, indicative of an efficient uptake of the drug carrier by tumor cells. This initial result is an encouraging indication that these peptide NTs are indeed suitable drug carriers. Future work will include the investigation of the aspect ratio, as well as the stability of the NTs against disassembly under varying conditions.

tubes formed from the cyclic peptide–polymer conjugate prior to drug attachment [CP-p(HEA_{58}-*co*-$CEMA_{10})_2$] were also tested on various ovarian cancer-cell lines and found to be nontoxic at concentrations up to 590 $\mu g\,mL^{-1}$ (Figure S10 in the Supporting Information). The cells were incubated with RAPTA-C and the cyclic peptide–polymer NTs with bound RAPTA-C. It should be noted here that the RAPTA-C drug is tightly bound to the polymer through the stable Ru–PTA coordinate bond and will not be released. Therefore, toxic effects will be affected by the whole macromolecular metal complex. The precise Ru content of the solution was measured using ICPMS and used to compare against equivalent concentrations of RAPTA-C. A significant decrease (ca. 10 times) in the half maximal inhibitory concentration (IC_{50}) value for NT's with bound RAPTA-C was found for both cell lines, compared with RAPTA-C alone (Table 1 and Figure 3). The higher toxicity of the drugs attached to the NT carrier is indicative of better cell uptake resulting in the delivery of larger amounts of RAPTA-C into the cells.

These initial IC_{50} effects are similar to the degradable polymeric micelles described in previous work.[19] However, based on work by Discher and co-workers, worm-like aggregates

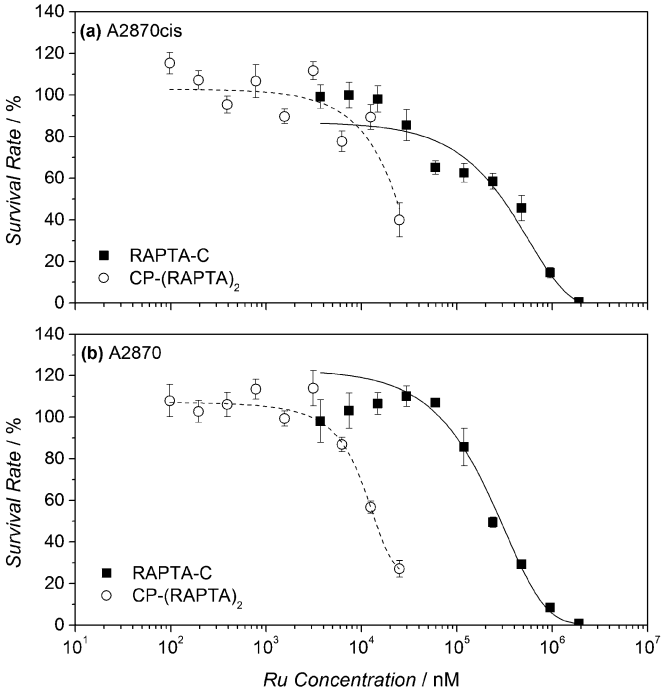

Figure 3. Cytotoxicity profile of RAPTA-C and CP-$(RAPTA)_2$ NTs, against ovarian carcinoma a) A2780 cells and b) A2780cis cells, after 72 h, $n = 4$. If the error bars are not visible, they fall into the data point.

Table 1. IC_{50} values of RAPTA-C and cyclic peptide–polymer NT-RAPTA-C, against ovarian A2780 and cisplatin-resistant ovarian A2780cis cancer-cell lines.

IC_{50} [μM]	A2780	A2780cis
RAPTA-C (literature)	353 ± 14 [20]	> 200 [21]
RAPTA-C	271	266
NT–RAPTA-C	15	22

Acknowledgements

The authors would like to thank Dr. Dorothy Yu for the ICPMS analyses at the Solid State & Elemental Analysis Unit, UNSW. Also, we like to thank Donald Thomas, at the Nuclear Magnetic Resonance Facility at UNSW, for his continued help and support. The authors would like to acknowledge the University of New South Wales and the Cooperative Research Centre for Polymers for scholarships for B.M.B., the Australian Government for the provision of a scholarship for R.C., and the Australian Research Council Discovery (M.D., K.A.J., and S.P., DP110101608) and Future Fellowship (M.H.S. FT0991273; S.P. FT120100536) programs.

Keywords: drug conjugation · nanotubes · peptides · ruthenium · self-assembly

[1] a) R. Duncan, *Nat. Rev. Cancer* **2006**, *6*, 688 – 701; b) R. Duncan, *Curr. Opin. Biotechnol.* **2011**, *22*, 492 – 501.
[2] A. Z. Wang, R. Langer, O. C. Farokhzad, *Ann. Rev. Med.* **2012**, *63*, 185 – 198.
[3] J. A. Champion, Y. K. Katare, S. Mitragotri, *J. Controlled Release* **2007**, *121*, 3 – 9.
[4] a) D. T. Bong, T. D. Clark, J. R. Granja, M. R. Ghadiri, *Angew. Chem.* **2001**, *113*, 1016 – 1041; *Angew. Chem. Int. Ed.* **2001**, *40*, 988 – 1011; b) R. Chapman, M. Danial, M. L. Koh, K. A. Jolliffe, S. Perrier, *Chem. Soc. Rev.* **2012**, *41*, 6023 – 6041.
[5] R. J. Brea, C. Reiriz, J. R. Granja, *Chem. Soc. Rev.* **2010**, *39*, 1448 – 1456.
[6] R. Chapman, G. G. Warr, S. Perrier, K. A. Jolliffe, *Chem. Eur. J.* **2013**, *19*, 1955 – 1961.
[7] a) R. Chapman, K. A. Jolliffe, S. Perrier, *Aust J Chem.* **2010**, *63*, 1169 – 1172; b) R. Chapman, K. A. Jolliffe, S. Perrier, *Polym. Chem.* **2011**, *2*, 1956 – 1963.
[8] R. Chapman, M. L. Koh, G. G. Warr, K. A. Jolliffe, S. Perrier, *Chem. Sci.* **2013**, *4*, 2581 – 2589.
[9] a) M. G. J. ten Cate, N. Severin, H. G. Börner, *Macromolecules* **2006**, *39*, 7831 – 7838; b) J. Couet, J. D. J. S. Samuel, A. Kopyshev, S. Santer, M. Biesalski, *Angew. Chem.* **2005**, *117*, 3361 – 3365; *Angew. Chem. Int. Ed.* **2005**, *44*, 3297 – 3301.
[10] M. J. Webber, J. A. Kessler, S. I. Stupp, *J. Intern. Med.* **2010**, *267*, 71 – 88.
[11] Y. Geng, P. Dalhaimer, S. Cai, R. Tsai, M. Tewari, T. Minko, D. E. Discher, *Nat. Nanotechnol.* **2007**, *2*, 249 – 255.
[12] H. Maeda, *Bioconjugate Chem.* **2010**, *21*, 797 – 802.
[13] Y. Wang, S. Yi, L. Sun, Y. Huang, S. C. Lenaghan, M. Zhang, *J. Biomed. Nanotechnol.* **2014**, *10*, 445 – 454.
[14] M. Callari, J. R. Aldrich-Wright, P. L. de Souza, M. H. Stenzel, *Progr. Polym. Sci.* **2014**, DOI: 10.1016/j.progpolymsci.2014.05.002
[15] a) C. S. Allardyce, P. J. Dyson, *Platinum Metals Rev.* **2001**, *45*, 62 – 69; b) A. Bergamo, A. Masi, P. J. Dyson, G. Sava, *Int. J. Oncol.* **2008**, *33*, 1281 – 1289; c) C. S. Allardyce, P. J. Dyson, D. J. Ellis, S. L. Heath, *Chem. Commun.* **2001**, 1396 – 1397; d) B. Wu, M. S. Ong, M. Groessl, Z. Adhireksan, C. G. Hartinger, P. J. Dyson, C. A. Davey, *Chem. Eur. J.* **2011**, *17*, 3562 – 3566; e) C. Scolaro, A. Bergamo, L. Brescacin, R. Delfino, M. Cocchietto, G. Laurenczy, T. J. Geldbach, G. Sava, P. J. Dyson, *J. Med. Chem.* **2005**, *48*, 4161 – 4171; f) C. Scolaro, T. J. Geldbach, S. Rochat, A. Dorcier, C. Gossens, A. Bergamo, M. Cocchietto, I. Tavernelli, G. Sava, U. Rothlisberger, P. J. Dyson, *Organometallics* **2005**, *24*, 756 – 765.
[16] S. Chatterjee, S. Kundu, A. Bhattacharyya, C. G. Hartinger, P. J. Dyson, *J Biol Inorg Chem.* **2008**, *13*, 1149 – 1155.
[17] P. J. Dyson, G. Sava, *Dalton Trans.* **2006**, 1929 – 1933.
[18] B. M. Blunden, D. S. Thomas, M. H. Stenzel, *Polym. Chem.* **2012**, *3*, 2964 – 2975.
[19] B. Blunden, H. Lu, M. H. Stenzel, *Biomacromolecules* **2013**, *14*, 4177 – 4188.
[20] C. K. Poon, R. Chapman, K. A. Jolliffe, S. Perrier, *Polym. Chem.* **2012**, *3*, 1820 – 1826.
[21] W. Xiang, Y. Zhou, X. Yin, X. Zhou, S. Fang, Y. Lin, *Electrochim. Acta* **2009**, *54*, 4186 – 4191.
[22] P. Servin, R. Laurent, L. Gonsalvi, M. Tristany, M. Peruzzini, J.-P. Majoral, A.-M. Caminade, *Dalton Trans.* **2009**, 4432 – 4434.
[23] A. D. Phillips, L. Gonsalvi, A. Romerosa, F. Vizza, M. Peruzzini, *Coord. Chem. Rev.* **2004**, *248*, 955 – 993.

Received: April 17, 2014
Published online on ■■ ■■, 0000

COMMUNICATION

Self-Assembly

B. M. Blunden, R. Chapman, M. Danial, H. Lu, K. A. Jolliffe, S. Perrier,* M. H. Stenzel**

■■ – ■■

Drug Conjugation to Cyclic Peptide–Polymer Self-Assembling Nanotubes

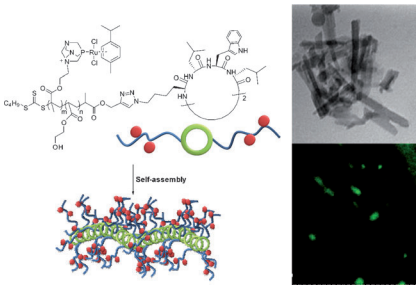

Polymeric nanotubes (NTs) based on self-assembled conjugates of polymers and cyclic peptides can be used as an efficient drug carrier for RAPTA-C, a ruthenium-based anticancer drug. The drug was conjugated to a water-soluble polymer, which formed the shell of the NTs. The self-assembled nanotubes (ca. 200–500 nm in length) had a significant activity against cancer cells (see figure).